

# Microstructure and morphology of $\alpha$ -Si:H solar cells grown on metallized flexible substrates

J. D. SAUNDERSON

*Department of Physics, Rand Afrikaans University, P.O. Box 524, Auckland Park 2006, South Africa*

M. J. WITCOMB\*

*Electron Microscope Unit, University of the Witwatersrand, Private Bag 3, WITS, 2050, South Africa*

*E-mail: mikew@gecko.biol.wits.ac.za*

R. SWANEPOEL

*Department of Physics, Rand Afrikaans University, P.O. Box 524, Auckland Park 2006, South Africa*

Results are presented for the microstructure of  $\alpha$ -Si:H solar cells grown on metallized polymer substrates. The structures studied were Kapton/metal/n-i-p  $\alpha$ -Si:H/ZnO, where silver and aluminum were used as the metal back contacts. The  $\alpha$ -Si:H was deposited at temperatures ranging from 100–200 °C. A second identical range of cells, except for the insertion of an 80 nm thick ZnO buffer-layer between the metal and n-layer, was also studied. A range of measurements utilising scanning electron microscopy, energy dispersive x-ray spectroscopy, Raman scattering and X-ray diffraction were made on the samples to determine the material properties. It is demonstrated that the surface morphology and microstructure of these cells are strongly dependent on the substrate temperature during deposition of the  $\alpha$ -Si:H, choice of back contact metal, and the ZnO buffer-layer. It is argued that the material properties of cells grown on flexible metallized substrates differ from those grown on conventional TCO covered glass substrates.

© 2001 Kluwer Academic Publishers

## 1. Introduction

Although the crystallization temperature of Si is  $\sim 900$  °C, it has been demonstrated that crystalline silicon is formed if  $\alpha$ -Si:H layers on Al substrates are annealed above  $\sim 450$  °C [1]. In contrast, silicon crystallization occurs at  $\sim 170$  °C for traditional  $\alpha$ -Si:H solar cells (on glass) with thermally evaporated Al back contacts [2]. It has also been found that, for  $\alpha$ -Si:H cells grown on transparent conductive oxide (TCO) covered glass with sputtered Al back contacts, the cells displayed nodules of  $\sim 1$   $\mu$ m diameter [3]. These nodules were identified as silicon protrusions under the aluminum layer. In contrast, a previous study [4] had shown that, while  $\alpha$ -Si:H with gold (Au) back contacts displayed the formation of snowflake-like island structures followed by lateral growth, the  $\alpha$ -Si:H with aluminum contacts displayed no island formation, and remained laterally homogeneous. X-ray diffraction (XRD) studies have shown that annealing of glass/n :  $\alpha$ -Si:H/Al samples above 300 °C produced both Al and Si crystalline peaks [5].

Khait and Weil [6] proposed a model which describes the enhancement of the crystallization of  $\alpha$ -Si:H due to the presence of a metal, especially metals not form-

ing silicides (e.g. Al and Ag). According to the model, short-lived large energy fluctuations (SLEFs) of atomic particles occur, which supply the particles with sufficient energy ( $E > kT$ ) to overcome the energy barrier to perform a diffusion-like jump. During such jumps of Si atoms, mobile electrons from the metal contact can become trapped, and this process is associated with the formation of crystalline nuclei. When inter-diffusion of Si and materials like Al and Ag occur, an enhanced rate of crystallization is expected, and consequently crystallization of the  $\alpha$ -Si:H can occur at relatively low temperatures.

Recently, it has been demonstrated that the inter-diffusion of Al and Si takes place at even lower temperatures of  $\sim 160$  °C in  $\alpha$ -Si:H solar cells grown on aluminumized polymer substrates, and that this inter-diffusion has a detrimental effect on the cell parameters [7]. In this study, it was also shown that the insertion of a thin ZnO buffer-layer between the  $\alpha$ -Si:H and Al resulted in less inter-diffusion and more efficient cells. It has been argued that the material properties of cells grown on thin metal films on polymer substrates differ from those of traditional cells grown on TCO covered glass [8].

\* Author to whom all correspondence should be addressed.

The aim of the present investigation was to study the effects on the surface morphology and microstructure of  $\alpha$ -Si:H films deposited at different temperatures on aluminum and silver back contact films on flexible, Kapton polymer solar cell substrates as well as on ZnO buffer-layers deposited on these metallized substrates. In addition, differences were looked for resulting from the silicon network being formed in the presence of a metal film in the flexible substrate case in contrast to TCO in the conventional case of rigid glass substrates.

## 2. Experimental

Flexible polymer substrates (Kapton<sup>R</sup>) were metallized with aluminum and silver by means of thermal evaporation. One half of these substrates were also covered with an 80 nm thick layer of ZnO by means of DC magnetron sputtering, to form a thin buffer-layer.  $\alpha$ -Si:H n, i, and p-layers were deposited (with thicknesses of 30 nm, 500 nm and 20 nm respectively) on the four sets of substrates at deposition temperatures  $T_s$  ranging from 100–200 °C in a large area, single chamber 13.56 MHz glow discharge deposition system. ZnO dots of 2 mm diameter were deposited onto these structures to define photovoltaic cells. Standard PH<sub>3</sub>, SiH<sub>4</sub> and B<sub>2</sub>H<sub>6</sub> gas mixtures were used with a hydrogen dilution of [SiH<sub>4</sub>]/[H<sub>2</sub>] = 0.6. A control “cell” was also grown on non-metallized Kapton at 200 °C for structural comparison with the cells grown on metallized Kapton.

Scanning electron microscopy (SEM) studies were undertaken on these samples in order to determine the morphology of the surfaces, while energy dispersive x-ray spectroscopy (EDS) analyses at 4–20 kV were performed on surface features to determine their chemical composition. XRD measurements were made on the complete cells to determine the microstructure of the materials, while Raman scattering measurements were taken on the silicon top surface of the complete cells to determine the degree of micro-crystallinity of the silicon.

## 3. Results

### 3.1. Morphology of native materials

SEM micrographs of the metallized polymer are shown in Fig. 1, along with the silicon top surface of the n-i-p:  $\alpha$ -Si:H structure grown on the non-metallized polymer. While the silicon surface appears almost featureless, the aluminized polymer displays separate but intersecting ridges, consisting of arrays of small humps or nodules. The ridges are separated by a grainy surface. The morphology of the silverized substrate, on the other hand, displays a much finer or smoother surface texture with no identifiable features. It is these samples of native materials against which the subsequent results are to be compared.

### 3.2. Morphology of $\alpha$ -Si:H

Scanning electron micrographs of the silicon top surface of the cells grown on Kapton/Al and Kapton/Ag are shown in Fig. 2 for a range of silicon deposition temper-

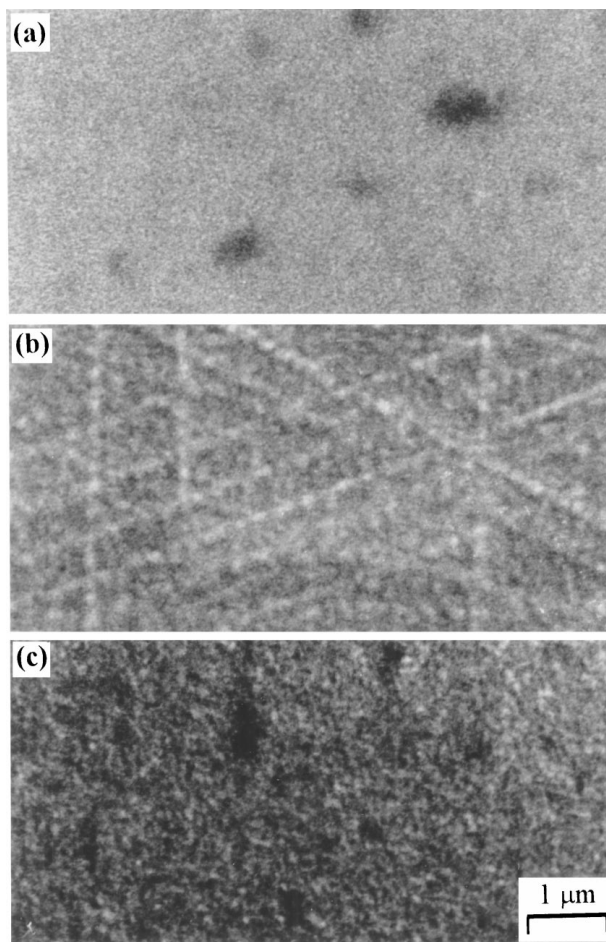


Figure 1 Scanning electron micrographs of the native materials: (a)  $\alpha$ -Si:H on non-metallized Kapton, (b) Kapton/Al and (c) Kapton/Ag.

atures  $T_s$ . It is clear, by comparing Fig. 2 to Fig. 1, that the silicon on the metallized Kapton exhibits a new morphology different to that of either of the native forms of the composite materials, even for a deposition temperature as low as 100 °C. This difference becomes more pronounced with increasing  $T_s$ .

For  $T_s = 100$  °C, the silicon appears grainy, but featureless on both the aluminized and silverized polymer. The ridges observed in the native aluminum were not transferred to the silicon during the deposition of the  $\alpha$ -Si:H. The silicon, deposited at 160 °C, however, displays distinct nodules of varying size. For the aluminized polymer, the  $\alpha$ -Si:H displays nodules of diameter of 300–500 nm on a grainy surface. On the silverized polymer, the silicon consists of densely packed nodules of  $\sim$ 200–300 nm diameter. The size of the nodules is larger for  $T_s = 200$  °C but, on the aluminized polymer, the silicon still consisted of nodules on a textured surface. It appears that the density (number per area) of the nodules remains constant for higher deposition temperatures. A high resolution image of the nodules of silicon, grown at 200 °C on the silverized polymer, is shown in Fig. 3. It is clearly demonstrated that a large differentiation in surface morphology is present on a scale of  $\sim$ 400 nm, which is indicative of a strong three-dimensional growth mechanism, as opposed to solely lateral growth. Also note the three pointed star shaped features on the nodules.

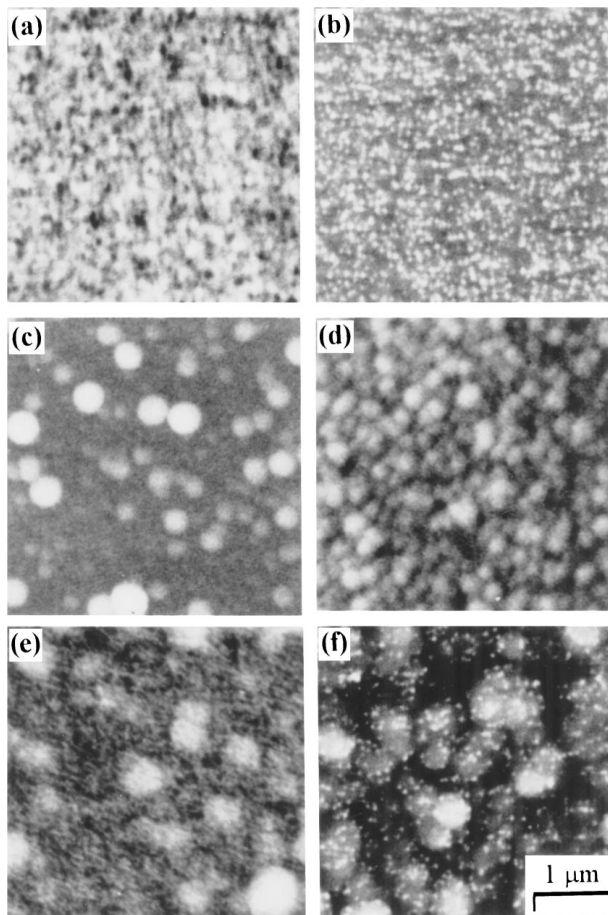


Figure 2 SEM micrographs of the  $\alpha$ -Si:H top surface of the cells grown at 100 °C on (a) Kapton/Al and (b) Kapton/Ag; grown at 160 °C on (c) Kapton/Al and (d) Kapton/Ag; grown at 200 °C on (e) Kapton/Al and (f) Kapton/Ag.

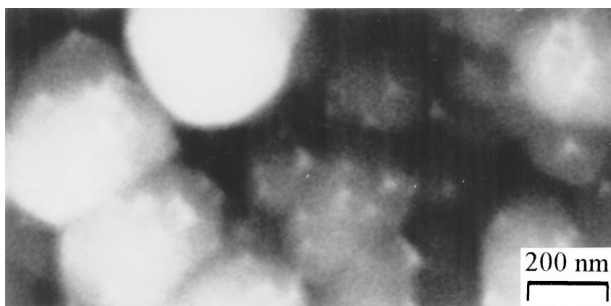


Figure 3 High resolution scanning electron micrograph of the silicon nodules, for the cell grown on silverized Kapton at 200 °C.

### 3.3. Chemical analyses

EDS was employed to undertake very localised analysis of individual nodules as well as of the areas between the nodules so as to investigate any differences in chemical composition due to a possible aggregation of specific materials to form the nodules. No evidence for such a chemical difference between the nodules and the background could, however, be found. The analyses indicated that the nodules, and the areas between them, consisted only of silicon, and no evidence for the presence of either Al or Ag at the surface was found, at least down to the minimum detection limit of 0.1 at.%. The size of the volumes analysed was down to  $0.027 \mu\text{m}^3$ . This figure corresponds to approximately  $0.3 \mu\text{m}$  diameter

regions which is the size of the larger nodules. The result of these analyses is supported by the Secondary Ion Mass Spectrometry (SIMS) and X-ray Photo-Emission Spectroscopy (XPS) measurements recently reported on larger integrated  $10\text{--}70 \mu\text{m}$  sided square analysed regions [7], which indicated that only small amounts (more than  $\sim 10^{16} \text{cm}^{-3}$  but less than  $\sim 0.1 \text{at.}\%$ ) of the back contact metal had diffused to the front surface of the cell.

### 3.4. Microstructure

Although crystallization of the  $\alpha$ -Si:H is not expected for low deposition temperatures in the region of 100–160 °C, XRD measurements were performed on all the samples. The results (see Fig. 4) indicate that the native aluminum on the Kapton is amorphous, but that the native silver on Kapton is micro-crystalline, displaying the silver (111), (200) and (220) peaks. The XRD measurements on the complete cell structures, however, indicate that the aluminum becomes micro-crystalline, displaying the aluminum (111) and (220) peaks, even for  $T_s = 100 \text{ °C}$ . The degree of crystallinity of the silver also increases when  $\alpha$ -Si:H is deposited onto it. Although XRD measurements of both samples

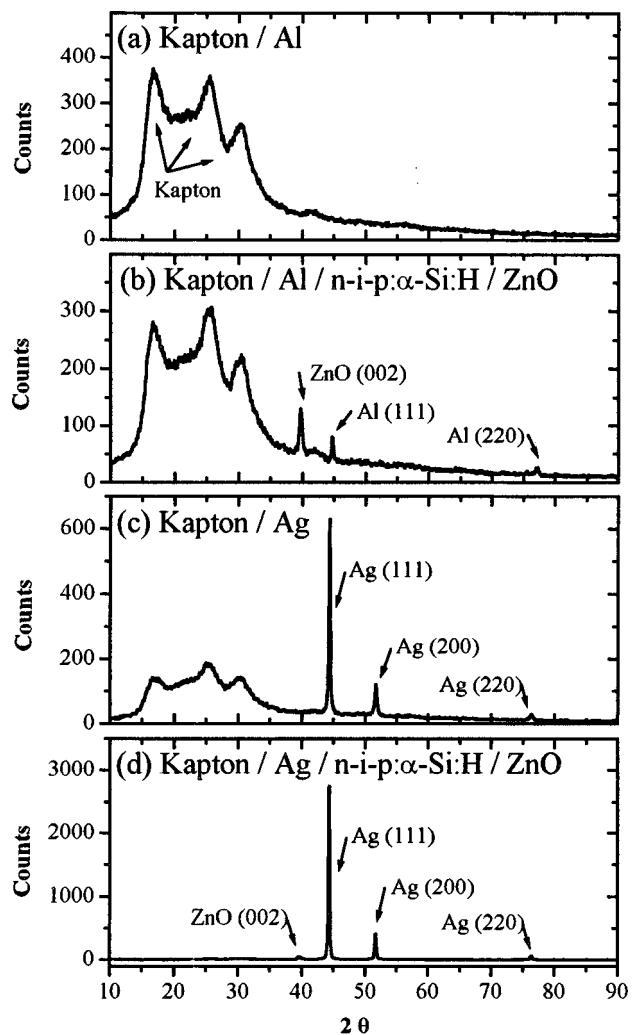


Figure 4 XRD spectra of the (a) as-deposited Kapton/Al, (b) the complete cell grown on Kapton/Al at 200 °C, (c) as-deposited Kapton/Ag, and (d) the cell grown on Kapton/Ag at 200 °C.

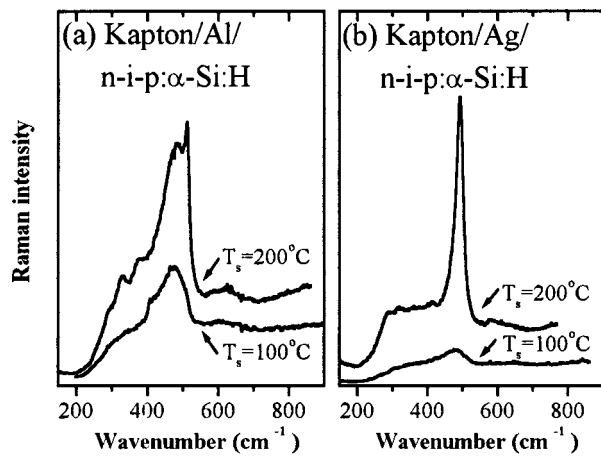


Figure 5 Raman spectra of the n-i-p silicon structures grown on (a) Kapton/Al and (b) Kapton/Ag, at 100 °C and 200 °C.

yielded the expected ZnO (002) peaks, no evidence for the crystallization of the  $\alpha$ -Si:H was found.

In contrast to this observation, the Raman spectra (Fig. 5) indicate that the  $\alpha$ -Si:H does become more crystalline at higher temperatures, and that the degree of crystallinity is higher for the silicon grown on the silverized polymer than for the aluminized polymer. All the evidence suggests that the silicon grown on the metallized substrates at 100 °C is amorphous, and that a degree of amorphous to crystalline transition occurs at temperatures between 160 to 200 °C.

### 3.5. Effect of buffer-layer

It has been recently demonstrated that the ZnO buffer-layer performs two important functions, that of impeding the inter-diffusion of the metal contact and  $\alpha$ -Si:H [7], and of causing a strong suppression of the amorphous to crystalline transition [8]. The insertion of this buffer-layer also has an effect on the morphology of the silicon deposited onto it, as shown in Fig. 6 for the cells grown at  $T_s = 100$  °C. By comparing Fig. 6 to Fig. 2a and b, it is clear that the silicon deposited onto the ZnO buffer-layer shows a rougher surface morphology than the silicon grown directly on the metal for  $T_s = 100$  °C. The cells with the buffer-layer for  $T_s = 100$  °C resemble the cells without the buffer-layer at 160 °C. It is also evident that the underlying metal layers still influence the morphology of the silicon, despite the presence of the buffer-layer between them.

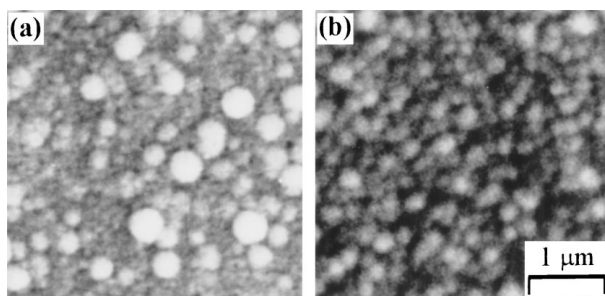


Figure 6 SEM micrographs of the  $\alpha$ -Si:H top surface of the cells grown on (a) Kapton/Al/ZnO and (b) Kapton/Ag/ZnO, at 100 °C.

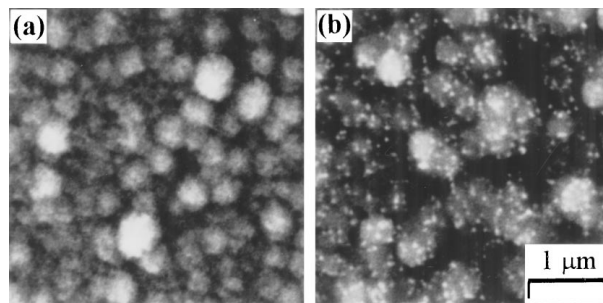


Figure 7 SEM micrographs of the ZnO window-layer grown on (a) Kapton/Al/n-i-p:  $\alpha$ -Si:H and (b) Kapton/Ag/n-i-p:  $\alpha$ -Si:H. The silicon was deposited at  $T_s = 100$  °C.

For higher deposition temperatures, the differences in morphology between the cells with and without the buffer-layer become less pronounced. Raman spectra performed on the cells grown on the buffer-layer, indicated that the silicon is amorphous, even at 200 °C [8]. Despite being amorphous, the silicon still displays the characteristic nodules.

### 3.6. Window layer

SEM micrographs of the ZnO window-layer are displayed in Fig. 7 for the cells grown at 100 °C. Although the window-layers were deposited simultaneously on these cells, the morphologies of the two ZnO surfaces differ. Both samples consist of nodules of varying size, and the nodules of ZnO on the Kapton/Al/n-i-p:  $\alpha$ -Si:H are smaller than those of the ZnO on Kapton/Ag/p-i-n:  $\alpha$ -Si:H. It is also clear that the differences in the morphologies of the underlying surfaces determine the morphologies of the window layers. For both substrates, the ZnO window-layers are micro-crystalline, displaying the ZnO (002) XRD peaks.

## 4. Discussion and conclusions

The main results of this study can be summarized as follows:

1. The native  $\alpha$ -Si:H is, indeed, amorphous, and appears almost featureless when grown on non-metallized Kapton.
2. The native aluminum is amorphous, while the native Ag is micro-crystalline. Both materials exhibit fairly smooth surfaces, with the Al displaying ridges, consisting of arrays of nodules, while the Ag remains featureless.
3. When silicon is deposited onto the aluminum and silver native films, both metal layers display micro-crystalline properties, even at low deposition temperatures around  $T_s = 100$  °C.
4. The  $\alpha$ -Si:H structures deposited onto the metal films are amorphous for  $T_s = 100$  °C, and become progressively more crystalline toward  $T_s \approx 160$ –200 °C. The degree of crystallinity of the silicon is higher for the cells grown on silver than on aluminum.
5. When silicon is deposited onto the metal films, the silicon consists of nodules, the size of which increases with increasing  $T_s$ . This behaviour is in

contrast to  $\alpha$ -Si:H films grown on glass which display a flat, featureless surface corresponding to high-quality  $\alpha$ -Si:H formed by lateral two-dimensional growth [9]. This morphology differs completely from either of the native forms of the constituent materials, despite the deposition conditions being identical.

6. The silicon structures grown on the buffer-layer (Kapton/metal/ZnO) also exhibit the nodule structures, but are amorphous for all deposition temperatures.

These results should be considered in context with known results from the literature. The relevant results are:

1. The majority of studies considered structures where the metal contacts were deposited onto an existing  $\alpha$ -Si:H network. In contrast, the samples reported on in this study consist of  $\alpha$ -Si:H layers (cells) grown on thin metal films. The difference is that during deposition of the  $\alpha$ -Si:H in the flexible cells, the  $\alpha$ -Si:H network is being formed in the presence of a metal film.

2. It is well known that the  $\alpha$ -Si:H/metal contact (metal deposited onto  $\alpha$ -Si:H) induces a range of phenomena: Crystallization of the  $\alpha$ -Si:H [1, 2, 5] and sometimes also the crystallization of the metal contact [6] (Al) with annealing at low temperatures ( $\sim 180$ – $300$  °C), and the formation of features like “snowflakes” [4] and nodules [3]. Si/Al inter-diffusion has been reported for  $\alpha$ -Si:H deposited on bulk Al [1].

3. When flexible cells are made (with Al deposited on  $\alpha$ -Si:H as opposed to conventional cells), the interactions between the metal film and  $\alpha$ -Si:H seem to result in enhanced occurrences of the above phenomena [7, 8].

The results presented here, indicate that not only the  $\alpha$ -Si:H, but also the metal is susceptible to crystallization, and even more so than the  $\alpha$ -Si:H since the aluminum, for example, becomes crystalline at lower temperatures than the  $\alpha$ -Si:H. Although the size of the nodules (of silicon) increase toward higher deposition temperatures, their mere existence cannot be attributed to the crystallization of the silicon. Indeed, a view more consistent with the observations would be that the nodules occur as a result of the crystalline nature of the metal films.

A simple model to describe the processes occurring in the flexible cells can be put forward: When  $\alpha$ -Si:H is deposited onto a metal film at elevated temperatures, the metal and silicon atoms interact strongly. Specifically, a large degree of inter-diffusion of these species occur. The extent of the inter-diffusion is larger for flexible cells than for conventional cells, since the metals (Al and Ag) are rather mobile in  $\alpha$ -Si:H, and the  $\alpha$ -Si:H is being formed in the presence of the metal film. Also, inter-diffusion of Al or Ag and Si occurs during Si deposition, so that metallic atoms diffuse deep into the  $\alpha$ -Si:H network. The flexibility of the substrate in contrast to a rigid glass substrate will introduce stress gradients within the  $\alpha$ -Si:H film which will enhance this diffusion. As Al and Ag are known not to form silicides, a large density of mobile electrons occur, and induce

nucleation and crystallization (or enhancement thereof) of the metal film even at low temperatures. The sites of nucleation serve to form an inhomogeneous substrate, and as the silicon layer becomes thicker during deposition, nodules of material grow from these sites. Between these islands, lateral growth of increasing numbers of layers of silicon occurs. At higher temperatures, this mechanism is enhanced and results in larger nodules and a larger degree of three dimensional growth. Concurrently, at higher temperatures, the known amorphous to crystalline transition starts occurring, and crystallites form within the Si network. These crystallites are incorporated in the nodules being formed during silicon growth.

The central peaked, three pointed star features found on the nodules of the films deposited on Kapton/Ag were a secondary observation of the study. The size of these features, typically 40 nm, precluded their analysis by SEM-EDS. Analysis by transmission electron microscopy, TEM-EDS, would be a logical choice since the features could totally occupy the analysed volume and lateral scattering of the electrons would be dramatically reduced due to the thinness of the section. However, thin foil sample preparation of such material to achieve this would be non-trivial. These features could be microcrystals since inter-diffusion of a metal can result in enhancement of the crystallization of  $\alpha$ -Si:H [6] and conditions would then be right for the realignment of the silicon around this nuclei. This viewpoint is given credence by the faceted nature of these features.

The Kapton surface was found to exhibit ridges on its surface. It is believed that the subsequent difference between the aluminium and silver coated Kapton surfaces may be a result of different growth kinetics. This is under investigation. The non-transference of the ridges in the native aluminium layers to the silicon layer is not understood. However, it would not necessarily be expected that the surface of the silicon layer would display the same morphology as the underlying substrate since the resulting surface morphology will be a function of the growth conditions and film thickness. For example, the deposition rate of the  $\alpha$ -Si:H was slow, about  $0.2 \text{ nm s}^{-1}$ . A short surface diffusion length would result in the  $\alpha$ -Si:H species not being able to find energetically favorable positions on the surface resulting in a strong 3-D, as opposed to lateral, growth.

The extent to which known phenomena, such as inter-diffusion, crystallization, and three dimensional growth take place in  $\alpha$ -Si:H solar cells grown on metallized polymer substrates has been found to be enhanced in comparison to traditional cells grown on TCO coated glass. This is due to the presence of a metal film while the silicon network is being formed rather than the metal being deposited after the silicon film in the glass substrate case. Since the use of flexible insulating substrates holds great promise for the commercialization of  $\alpha$ -Si:H solar cells through their lower cost/watt, these phenomena must be thoroughly understood since they will influence the quality and efficiency of the device: Our results indicate that the growth of Si on a metal, as opposed to the usual glass substrate, is inherently conducive to relatively lower quality  $\alpha$ -Si:H devices. The future challenge will be the engineering of such

materials so that the unwanted phenomena are suppressed, or perhaps even to make use of the occurrence of these phenomena in new cell structures.

### Acknowledgements

One of the authors (MJW) wishes to thank the University of the Witwatersrand for financial support via the Microstructural Studies Research Programme.

### References

1. S. J. JONES, A. B. SWARTZLANDER-FRANZ, Y. CHEN and D. L. WILLIAMSON, *Mat. Res. Soc. Symp. Proc.* **297** (1993) 1049.
2. M. S. HAQUE, H. A. NASEEM and W. D. BROWN, in Proceedings of the 1st World Conference on Photovoltaic Energy Conversion, Hawaii (1994) p. 642.

3. F. WILLING, M. BENNETT and J. NEWTON, in Proceedings of the 10th IEEE Photovoltaic Specialist Conference, New York (1987) p. 1086.
4. C. C. TSAI, R. J. NEMANICH, M. J. THOMSON and B. L. STAFFORD, *Physica* **117B & 118B** (1983) 953.
5. YU. L. KHAIT and R. WEIL, *J. Appl. Phys.* **78** (1995) 6504.
6. S. ISHIHARA, M. KITAGAWA and T. HIRAO, *ibid.* **62** (1987) 837.
7. J. D. SAUNDERSON, R. SWANEPOEL and M. J. VAN STADEN, *Solar Energy Materials & Solar Cells* **51** (1998) 425.
8. J. D. SAUNDERSON and R. SWANEPOEL, *ibid.* **53** (1998) 329.
9. J. D. SAUNDERSON, A. P. GREEF, H. C. SWART, C. M. DEMANET, D. F. LANGA, K. V. SANKAR and R. SWANEPOEL, in Proceedings of the 37th Conference of the Microscopy Society of Southern Africa, Johannesburg (1998) p. 7.

*Received 18 August 1997  
and accepted 21 June 2000*